REFLECTION SYMMETRY DETECTION BY EMBEDDING SYMMETRY IN A GRAPH

Rajendra Nagar and Shanmuganathan Raman

Electrical Engineering, Indian Institute of Technology Gandhinagar, India
{rajendra.nagar, shanmuga}@iitgn.ac.in

ABSTRACT

Reflection symmetry is ubiquitous in nature and plays an important role in object detection and recognition tasks. Most of the existing methods for symmetry detection extract and describe each keypoint using a descriptor and a mirrored descriptor. Two keypoints are said to be mirror symmetric keypoints if the original descriptor of one keypoint and the mirrored descriptor of the other keypoint are similar. However, these methods suffer from the following issue. The background pixels around the mirror symmetric pixels lying on the boundary of an object can be different. Therefore, their descriptors can be different. However, the boundary of a symmetric object is a major component of global reflection symmetry. We exploit the estimated boundary of the object and describe a boundary pixel using only the estimated normal of the boundary segment around the pixel. We embed the symmetry axes in a graph as cliques to robustly detect the symmetry axes. We show that this approach achieves state-of-the-art results in a standard dataset.

Index Terms— Reflection Symmetry, Graph, Cliques.

1. INTRODUCTION

An object is called reflective symmetric if it remains the same after reflecting it about its symmetry axis. Symmetry has various applications in computer vision such as image matching and recognition [1], face verification [2], and image editing [3]. We want to find the global reflection symmetry axes of symmetric objects present in a digital image. This problem has been attempted previously and promising results have been obtained through various approaches. The main theme of many existing methods, e.g., [4, 5, 6], is the following. Detect the keypoints and describe each keypoint using a descriptor (SIFT [7]) and a mirrored descriptor ([4]). Two keypoints are said to be mirror symmetric keypoints if the original descriptor of one keypoint and the mirrored descriptor of the other keypoint are similar. Then, each pair votes in the symmetry axis parameter space. The symmetry axis with maximum votes is the global symmetry axis. However, the keypoint detection based methods suffer from the following issue. The background pixels around the mirror symmetric pixels lying on the boundary of an object can be different. Therefore, their descriptors, such as SIFT descriptors, can be different. Hence, the boundary keypoints can not be used for symmetry detection. However, the boundary of a symmetric object is a major component of global reflection symmetry.

We use the fact that reflection symmetry of an object is mainly defined by its boundary. Finding perfect boundaries is a hard problem as the boundaries of non-symmetric objects are also detected. This makes the direct matching of boundaries approach to be ineffective. We construct a graph where each node represents a pair of symmetric pixels and two vertices share an edge if the symmetry axes defined by the corresponding pairs are similar. We observe that a symmetry axis corresponds to a clique in this graph. We detect all the symmetry axes iteratively by detecting the dominant cliques. Our main contributions in this work are the following.

1. A novel boundary orientation based method for detecting pairs of reflection symmetric pixels.
2. Construction of a graph where each reflection symmetry axis is embedded as a clique.
3. Detection of the symmetry axes by finding all the dominant cliques. This approach is robust, since by considering only the dominant cliques, we never consider the outlier boundaries while finding the symmetry axes.

2. RELATED WORK

The problem of detecting symmetry axis of all the symmetric objects present in an image has been an active research problem in computer vision and image processing. The recent challenges organized for symmetry detection in the real world images are [9, 10, 8]. Various approaches for symmetry detection in digital images are reviewed in [11]. The approaches for reflection symmetry detection in real-world images can be categorized as *voting based* approaches [12, 13, 14, 21, 4, 6, 5, 15, 16, 17] and multiple model fitting approaches in [18, 19, 20]. The voting based approaches are near invariant to noise. However, due to the voting procedure, they are time-consuming. Loy and Eklundh described each keypoint by SIFT and mirrored SIFT descriptors and used the Hough

R. Nagar was supported by a TCS Research Scholarship and S. Raman was supported by a SERB Core Research Grant.

transform based line detection algorithm [4]. This method relies on the detection of keypoionts within the boundaries of the symmetric object. Atadjanov *et al.* detected symmetry axes using the appearance of structure features. Each edge point is described by the curvature at the point of intersection of the edge passing through the point and the circle centered at this point [6]. They did not use the edge features within the circle. Elawady *et al.* proposed an efficient voting based method, where they used the edge characteristics in the Log-Gabor wavelet response space [5]. However, the Log-Gabor response at mirror symmetric pixels lying on the boundaries can be different due to different backgrounds. Therefore, boundary pixels may not participate in the symmetry detection process. Bokeloh *et al.* performed matching of locally coherent constellations of feature lines to detect the rigid symmetries [22]. Cornelius *et al.* used feature descriptors that are robust to local affine distortion to find the symmetric feature pairs [23]. Cicconet *et al.* proposed a registration based approach for single axis detection [26]. However, this approach can not detect multiple symmetry axes.

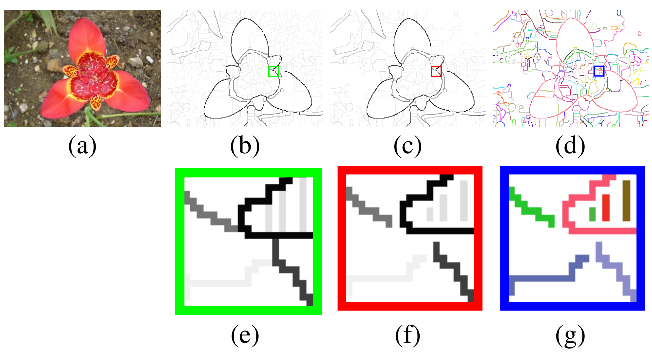

Fig. 1: Preprocessing of boundary map. (a) Input image, (b) UCM, (c) removing junctions to make boundaries valid curves, (d) the extracted dominant boundary from the cluttered boundary map, (e) zoomed UCM, (f) zoomed UCM after junctions removal, and (g) zoomed dominant boundary.

3. PROPOSED APPROACH

3.1. Detecting Pairs of Reflective Symmetric Pixels

The most important step of the symmetry axis detection is to find the pairs of pixels which are mirror reflections of each other. Our main observation is that the global reflection symmetry of an object is mainly defined by its boundary. We describe each boundary pixel using the orientation of the boundary segment passing through the pixel. Therefore, our first step is to automatically detect the object boundary. We use the method in [24] to find the boundary map of an image.

Let I be the input image. We represent the boundary map as ultrametric contour map (UCM). Let E be the boundary map. We observe that the boundary of the symmetric object is connected to the various other outlier boundaries as depicted in Fig. 1(b), (e). We describe each pixels using the boundary segment (represented as a curve) passing through it. Hence, we first preprocess the UCM boundary map such that the boundaries of the objects can be represented as curves, i.e., no branchings. We first detect the junction pixels which are the pixels such that the boundary strength is maximum in the 3×3 neighborhood and the number of pixels in the 3×3 neighborhood for which the boundary map has non-zero value is greater than or equal to 4. Then, to be able to represent a boundary as a curve, we set the boundary strength to zero for pixels in the 3×3 neighborhood of the junction pixels which have the boundary score to be non-zero and the boundary strength is not maximum. In Fig. 1 (c), (f), we show this step. We observe that we are able to extract the complete boundary of the object which can be represented as a curve, i.e., no branching, from the cluttered outlier boundaries. Further, let $\mathcal{F}$ be the set of all boundary pixels. The boundary map may not contain the complete boundary of the symmetric object due to occlusions and noise. Therefore, we consider a fixed length boundary segment around each pixel.

To find the pairs of reflection symmetric pixels, we first describe each boundary pixel $\mathbf{p}_i \in \mathcal{F}$ by using the normals of the boundary segment passing through the pixels $\mathbf{p}_i$. Let $b_i : [0,1] \rightarrow \mathcal{F}$ be the boundary segment of length z pixels (represented as curve) passing through the pixel $\mathbf{p}_i$ such that $b_i(0.5) = \mathbf{p}_i$, where $\mathbf{p}_i$ is the mid-point of the boundary segment curve b_i. If the two pixels $\mathbf{p}_i$ and $\mathbf{p}_{i'}$ are mirror reflections of each other, then they define a symmetry axis. Now, let $\mathbf{n}_i(t)$ be the normal to the curve b_i and $\mathbf{n}_{i'}(t)$ be the normal to the curve $b_{i'}$ at t. Further, let b_i^{r} be the reflection of the curve b_i about the symmetry axis defined by the pair of pixels $\mathbf{p}_i$ and $\mathbf{p}_{i'}$. Then, it is easy to observe that the angle between the normal $\mathbf{n}_i^{\mathrm{r}}(t)$ to the curve b_i^{r} at t and the normal $\mathbf{n}_{i'}(t)$ to the curve b_i' at t should be equal to $0°$ for all $t \in [0,1]$. Similarly, let $b_{i'}^{\mathrm{r}}$ be the reflection of the curve $b_{i'}$ about the symmetry axis defined by the pair of pixels $\mathbf{p}_i$ and $\mathbf{p}_j$.Then, the angle between the normal $\mathbf{n}_{i'}^{\mathrm{r}}(t)$ to the curve b_i^{r} at t and the normal $\mathbf{n}_i(t)$ to the curve b_i at t should be equal to $0°$ for all $t \in [0,1]$. Therefore, the pixels $\mathbf{p}_i$ and $\mathbf{p}_{i'}$ form a pair of reflection symmetric pixels, if Eq.(1) is satisfied.

$$\int_0^1 \cos^{-1}\left((\mathbf{n}_i^{\mathrm{r}}(t))^\top \mathbf{n}_{i'}(t)\right) + \cos^{-1}\left((\mathbf{n}_{i'}^{\mathrm{r}}(t))^\top \mathbf{n}_i(t)\right) dt = 0. \quad (1)$$

For the case of perfect symmetry, Eq.(1) holds true. However, due to the presence of noise and illumination variations, this might not hold true in practice. Therefore, we say that the pixels $\mathbf{p}_i$ and $\mathbf{p}_j$ form a pair of reflection symmetric pixels if $\int_0^1 \cos^{-1}\left((\mathbf{n}_i^{\mathrm{r}}(t))^\top \mathbf{n}_{i'}(t)\right) + \cos^{-1}\left((\mathbf{n}_{i'}^{\mathrm{r}}(t))^\top \mathbf{n}_i(t)\right) dt < \theta$. We chose $\theta = 5°$ in all our experiments. In Fig.2, we show a graphical illustration of the curve reflection process and the measurement of the similarity between the normals.

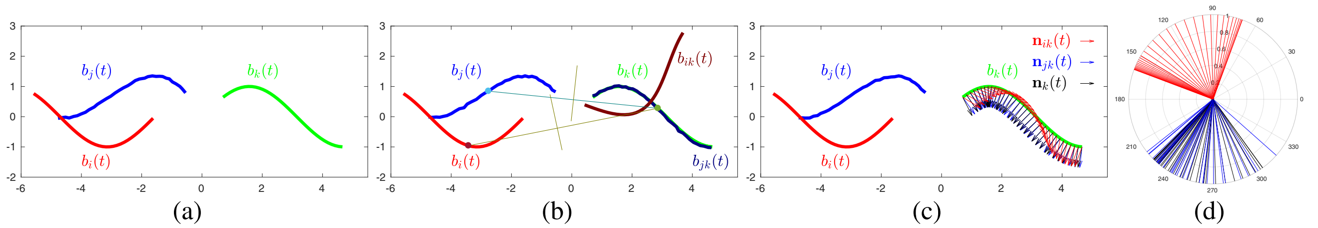

Fig. 2: Illustration of pairs of mirror symmetric pixels detection approach. (a) Three curves $b_i(t)$, $b_j(t)$, and $b_k(t)$. (b) Reflection of the curves $b_i(t)$, $b_j(t)$ about the symmetry axes L_{ki} and L_{ji} defined by the pairs (b_k, b_i) and (b_k, b_j), respectively. (c), (d) The normals $\mathbf{n}_{ki}$, $\mathbf{n}_{kj}$, $\mathbf{n}_k$ to the curves b_{ki}, b_{kj}, and b_k, respectively, shown on the curve b_k for better comparison.

3.2. Detecting Reflection Symmetry Axes

Our goal is to detect all the symmetry axes using the set of detected pairs of mirror symmetric pixels which possibly contain outlier pairs. First, we cluster the pairs of mirror symmetric pixels. Then, we find the symmetry axis in each cluster separately. Let $\{(\mathbf{p}_i, \mathbf{p}_{i'})\}_{i=1}^{f}$ be the detected f pairs of mirror symmetric pixels. We construct an undirected graph $\mathcal{G} = (\mathcal{V}, \mathcal{E})$, where each vertex v_i in the vertex set $\mathcal{V}$ corresponds to the pair $(\mathbf{p}_i, \mathbf{p}_{i'})$. We connect the vertices v_i and v_j by an unit weight edge if the symmetry axes L_i and L_j, defined by the pairs $(\mathbf{p}_i, \mathbf{p}_{i'})$ and $(\mathbf{p}_j, \mathbf{p}_{j'})$ respectively, are similar. We define the similarity between the symmetry axes as follows. Let b^{r}_{ji} be the reflection of the curve b_j through the symmetry axis L_i and $\mathbf{n}^{\mathrm{r}}_{ji}(t)$ be its normal at t. Similarly, let b^{r}_{ij} be the reflection of the curve b_i through the symmetry axis L_j and $\mathbf{n}^{\mathrm{r}}_{ij}(t)$ be its normal at t. If the symmetry axes L_i and L_j are similar, then the angle between the normals $\mathbf{n}^{\mathrm{r}}_{ji}(t)$ and $\mathbf{n}_{j'}(t)$ should be equal to $0°$ and the angle between the normals $\mathbf{n}^{\mathrm{r}}_{ij}(t)$ and $\mathbf{n}_{i'}(t)$ should be equal to $0°$. Therefore, we create an edge between the vertices v_i and v_j, if $\int_0^1 \cos^{-1}\left((\mathbf{n}^{\mathrm{r}}_{ji}(t))^\top \mathbf{n}_{j'}(t)\right) + \cos^{-1}\left((\mathbf{n}^{\mathrm{r}}_{ij}(t))^\top \mathbf{n}_{i'}(t)\right) dt < \theta$.

We observe that each clique in the graph $\mathcal{G}$ corresponds to the set of pairs of mirror symmetric pixels belonging to the same symmetry axis. We further, observe that each outlier pair does not make an edge with any other pairs. The outlier pairs remain isolated vertices in the graph $\mathcal{G}$. Therefore, our goal is to find the first k dominant cliques of the graph $\mathcal{G}$ in order to find all the k reflection symmetry axes of an input images. However, finding clique in a graph is an NP-complete problem, hence we find the approximate solution as follows. A clique in the graph $\mathcal{G}$ is a subset $\mathcal{C}$ of the vertex set $\mathcal{V}$ such that every pair of vertices in $\mathcal{C}$ are connected by an edge. It is a well known result that a clique is equivalent to an independent set in the complement graph of the graph $\mathcal{G}$ [25]. The complement graph $\bar{\mathcal{G}} = (\bar{\mathcal{V}}, \bar{\mathcal{E}})$ of the graph $\mathcal{G}$ is the graph such that $\bar{\mathcal{V}} = \mathcal{V}$, $(u, v) \in \mathcal{E} \Rightarrow (u, v) \notin \bar{\mathcal{E}}$, and $(u, v) \notin \mathcal{E} \Rightarrow (u, v) \in \bar{\mathcal{E}}$. An independent set in the graph $\bar{\mathcal{G}}$ is a subset $\mathcal{I}$ of the vertex set $\bar{\mathcal{V}}$ such that no two vertices in $\mathcal{I}$ are adjacent. Furthermore, the independent set is the complement of the vertex cover [25]. A vertex cover of an undirected graph $\bar{\mathcal{G}}$ is a subset $\mathcal{V}_{\mathrm{c}}$ of vertices of $\bar{\mathcal{V}}$ such that if (v_i, v_j) is an edge in $\bar{\mathcal{G}}$, then either $v_i \in \bar{\mathcal{V}}$ or $v_j \in \bar{\mathcal{V}}$ or both $v_i, v_j \in \bar{\mathcal{V}}$. We solve the following integer linear program (ILP) to find the minimum vertex cover.

$$\begin{aligned} &\min \ \textstyle\sum_{v \in \bar{\mathcal{V}}} x_v \\ \text{s.t.} \quad & x_u + x_v \geq 1 \quad \forall (u, v) \in \bar{\mathcal{E}} \\ & x_v \in \{0, 1\} \quad\ \ \forall v \in \bar{\mathcal{V}} \end{aligned} \tag{2}$$

Here, the binary variable x_v is equal to 1, if the vertex v is in the vertex cover $\mathcal{V}_{\mathrm{c}}$ and is equal to 0, otherwise. The constraint $x_u + x_v \geq 1$ ensures that at least one vertex of the edge $(u, v) \in \bar{\mathcal{E}}$ is included in the vertex cover. We rewrite the above ILP in the standard form as shown in Eq. (3).

$$\min_{\mathbf{x}} \mathbf{1}^\top \mathbf{x} \text{ subject to } \mathbf{E}\mathbf{x} \geq 1, \quad \mathbf{x} \in \{0, 1\}^{|\bar{\mathcal{V}}|}. \tag{3}$$

Here, $\mathbf{1}$ is a vector of size $|\bar{\mathcal{V}}|$ with all elements equal to 1. The matrix $\mathbf{E} \in \{0, 1\}^{|\bar{\mathcal{E}}| \times |\bar{\mathcal{V}}|}$ is the edge incident matrix such that $\mathbf{E}(e, v) = 1$, if the e-th edge is incident on the vertex v and $\mathbf{E}(e, v) = 0$, if the e-th edge is not incident on the vertex v. The vertex cover problem is an NP-hard problem. Therefore, we use the best known approximation which is a 2-approximation obtained by relaxing the integer linear program in Eq. 3 to a linear program. In the relaxed program, each variable takes value in $[0, 1]$, i.e., $\mathbf{x} \in [0, 1]^{|\bar{\mathcal{V}}|}$. We obtain the final solution by an optimal thresholding approach. If $x_i \geq 0.5$, then $x_i = 1$. Otherwise, $x_i = 0$. Let $\mathcal{V}_{\mathrm{c}}$ be the vertex cover found. Then, the independent set $\mathcal{I} = \bar{\mathcal{V}} \backslash \mathcal{V}_{\mathrm{c}}$ and the clique $\mathcal{C} = \mathcal{I}$. We remove all the vertices of the clique $\mathcal{C}$ from the graph $\mathcal{G}$ and all the edges incident on them. Then, we find the next dominant clique in the remaining graph. We find the first k dominant cliques by following the above procedure. We present the complete procedure in Algorithm 1.

We use the detected pairs of reflective pixels to detect the symmetry axes. We represent the detected pairs of mirror symmetric pixels as the collection of sets $\{\mathcal{P}_i\}_{i=1}^{k}$ such that each set $\mathcal{P}_i$ contains pairs of mirror symmetric pixels which are symmetric about the same axis. Each pair $(\mathbf{p}_j, \mathbf{p}_{j'}) \in \mathcal{P}_i$ defines its own symmetry axis which is the line passing through the point $\frac{\mathbf{p}_j + \mathbf{p}_{j'}}{2}$ and is perpendicular to the vector

Algorithm 1 *Reflection Symmetry Detection*

Input: Image I, Number of symmetry axes k.

Find the boundary map from image I and preprocess it such that each boundary can be represented as a curve.
Find the pairs of reflective symmetric pixels.
Construct the graph $\mathcal{G}$.
for $i \in \{1, 2, \ldots, k\}$ **do**
  Construct complement graph $\bar{\mathcal{G}}$ of graph $\mathcal{G}$.
  Find minimum vertex cover $\mathcal{V}_c$ of $\bar{\mathcal{G}}$ by using Eq. (3).
  $\mathcal{I} = \bar{\mathcal{V}} \backslash \mathcal{V}_c$.
  $\mathcal{P}_i = \{(\mathbf{p}_j, \mathbf{p}_{j'}) : j \in \mathcal{I}\}$.
  Remove vertices $\mathcal{I}$ from the graph $\mathcal{G}$ and edges incident on them.
end for
k sets of pairs of mirror symmetric pixels $\{\mathcal{P}_i\}_{i=1}^{k}$.
Find the symmetry axis for each set separately.

Output: Detected reflection symmetry axes.

$\mathbf{p}_j - \mathbf{p}_{j'}$. Since all the pairs in the set $\mathcal{P}_i$ belongs to the same symmetry axis, the symmetry axes defined by all these pairs should be similar. Hence, the best symmetry axis which is close to all the candidate symmetry axes, is the average line passing through the point $\sum_{(\mathbf{p}_j, \mathbf{p}_{j'}) \in \mathcal{P}_i} \frac{\mathbf{p}_j + \mathbf{p}_{j'}}{2|\mathcal{P}_i|}$ and is perpendicular to the vector $\sum_{(\mathbf{p}_j, \mathbf{p}_{j'}) \in \mathcal{P}_i} (\mathbf{p}_j - \mathbf{p}_{j'})$.

4. RESULTS AND EVALUATION

We have used the standard benchmark dataset in [8] to test and evaluate our method. In Fig. 3, we present a few examples of the detected symmetry axes on images from the dataset in [8] by the proposed approach. Two mirror symmetric boundary segments are shown in green color and connected by blue lines. The detected symmetry axes are shown in red color. We observe that the symmetry detected in all these examples is due to the pairs of reflective symmetric boundary pixels.

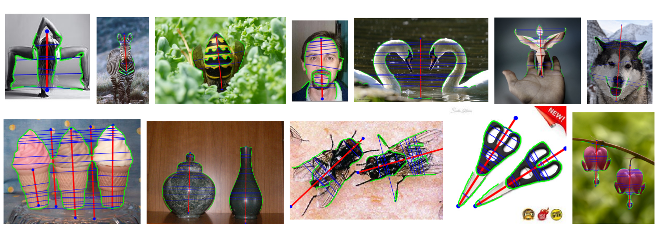

Fig. 3: Results on the dataset in [8]. First row: Single symmetry axis. Second row: Multiple symmetry axes.

We compare our method with the state-of-the-art methods [5], [26], [4], and [18] for single symmetry axis detection and with the methods [5], [4], and [18] for the multiple symmetry axes detection on the dataset in [8]. The method by [26] can only detect a single symmetry axis. Therefore, we do not compare with [26] for the multiple symmetry case. We use the metrics F-score and precision vs recall curves used in [8] to compute the precision and recall values. The F-score is defined as $F = \frac{2tp}{2tp+fp+fn}$, where, tp = number of correctly detected axes, fp = number of incorrectly detected axes, and fn = number of undetected ground-truth axes. Let ℓ_g be the ground truth symmetry axis. Similarly, let ℓ_e be the estimated symmetry axis. Then, the detected symmetry axis ℓ_e is correct if the angle between the lines ℓ_g and ℓ_e is less than θ_t, and the distance between the center points of the line segments ℓ_g and ℓ_e is less than the threshold d_t. We choose $d_t = 0.025 \times \min(w, h)$, $\theta_t = 3°$, and $z = 32$ pixels. Here, w and h are the width and height of the input image, respectively. For the case of multiple symmetry axes, we count only one correct detection if there are multiple correct detections for a single ground truth symmetry axis. In Fig. 4, we show the recall vs precision curves and the maximum F-score, represented as a big point on each curve, for all the methods. We observe that the proposed approach achieves the state-of-the-art performance on the dataset in [8] for multiple symmetry axes and the second-best performance for single symmetry axis.

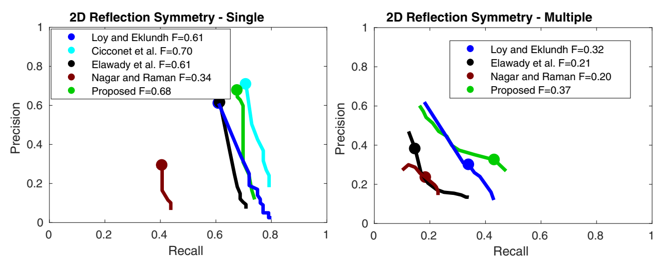

Fig. 4: Recall vs Precision curves for Elawady *et al.* [5], Cicconet *et al.* [26], Loy and Eklundh [4], Nagar and Raman [18], and the proposed approach on the dataset [8]. We report the maximum F-score values in the legends.

5. CONCLUSION AND FUTURE WORK

In this work, we have presented an efficient method for the detection of reflection symmetry axes for all the symmetric objects present in the given image. We have used the fact that the boundary of a symmetric object significantly determines the global reflection symmetry of a symmetric object. We have embedded the reflection symmetry in the graph, where each clique in the graph corresponds to a particular symmetry axis. We have achieved state-of-the-art performance on the standard benchmark dataset for multiple symmetry axes and second-best performance for single symmetry axis detection. Our method has a clear advantage over the keypoint based methods. Our method completely relies on the boundary detection. In future, we would like to improve the detected boundaries and the reflection symmetry detection by coupling both boundary and symmetry detection together.

References

[1] Daniel Cabrini Hauagge and Noah Snavely, "Image matching using local symmetry features," in *IEEE CVPR, 2012*, pp. 206–213.

[2] Charles Beumier and Marc Acheroy, "Face verification from 3d and grey level clues," *Pattern recognition letters*, vol. 22, no. 12, pp. 1321–1329, 2001.

[3] Michal Lukáč, Daniel Sýkora, Kalyan Sunkavalli, Eli Shechtman, Ondřej Jamriška, Nathan Carr, and Tomáš Pajdla, "Nautilus: Recovering regional symmetry transformations for image editing," *ACM Transactions on Graphics*, vol. 36, no. 4, 2017.

[4] Gareth Loy and Jan-Olof Eklundh, "Detecting symmetry and symmetric constellations of features," *ECCV 2006*, pp. 508–521.

[5] Mohamed Elawady, Christophe Ducottet, Olivier Alata, Cécile Barat, and Philippe Colantoni, "Wavelet-based reflection symmetry detection via textural and color histograms: Algorithm and results," in *IEEE ICCV Workshops 2017*, pp. 1734–1738.

[6] Ibragim R Atadjanov and Seungkyu Lee, "Reflection symmetry detection via appearance of structure descriptor," in *ECCV 2016*, Springer, pp. 3–18.

[7] David G Lowe, "Distinctive image features from scale-invariant keypoints," *International Journal of Computer Vision*, vol. 60, no. 2, pp. 91–110, Springer, 2004.

[8] Christopher Funk, Seungkyu Lee, Martin R. Oswald, Stavros Tsogkas, Wei Shen, Andrea Cohen, Sven Dickinson, and Yanxi Liu, "2017 iccv challenge: Detecting symmetry in the wild," in *IEEE ICCV Workshops 2017*.

[9] I Rauschert, J Liu, and Y Liu, "Symmetry detection competition: A summary of how the competition is carried out," in *IEEE CVPR Workshops*, 2011, pp. 1–66.

[10] Jingchen Liu, George Slota, Gang Zheng, Zhaohui Wu, Minwoo Park, Seungkyu Lee, Ingmar Rauschert, and Yanxi Liu, "Symmetry detection from realworld images competition 2013: Summary and results," in *IEEE CVPR Workshops*, 2013, pp. 200–205.

[11] Yanxi Liu, Hagit Hel-Or, Craig S Kaplan, and Luc Van Gool, "Computational symmetry in computer vision and computer graphics," *Foundations and Trends in Computer Graphics and Vision*, vol. 5, no. 1-2, pp. 1–195, 2010.

[12] Raymond KK Yip, "A hough transform technique for the detection of reflectional symmetry and skew-symmetry," *Pattern Recognition Letters*, vol. 21, no. 2, pp. 117–130, 2000.

[13] Viorica Patraucean, Rafael Grompone von Gioi, and Maks Ovsjanikov, "Detection of mirror-symmetric image patches," *IEEE CVPR Workshops*, 2013, pp. 211–216.

[14] Stavros Tsogkas and Iasonas Kokkinos, "Learning-based symmetry detection in natural images," in *ECCV*. Springer, 2012, pp. 41–54.

[15] Eckart Michaelsen and Michael Arens, "Hierarchical grouping using gestalt assessments," in *IEEE ICCV Workshops*, 2017, vol. 3, p. 5.

[16] Quanyi Mo and Bruce Draper, "Detecting bilateral symmetry with feature mirroring," in *IEEE CVPR Workshops*, 2011.

[17] Zhaozhong Wang, Zesheng Tang, and Xiao Zhang, "Reflection symmetry detection using locally affine invariant edge correspondence," *IEEE Transactions on Image Processing*, vol. 24, no. 4, pp. 1297–1301, 2015.

[18] Rajendra Nagar and Shanmuganathan Raman, "Reflection symmetry axes detection using multiple model fitting," *IEEE Signal Processing Letters*, vol. 24, no. 10, pp. 1438–1442, 2017.

[19] Rajendra Nagar and Shanmuganathan Raman, "Symmmap: Estimation of the 2-d reflection symmetry map and its applications," in *IEEE ICCV Workshops*, 2017.

[20] Yansheng Ming, Hongdong Li, and Xuming He, "Symmetry detection via contour grouping," in *IEEE ICIP*, 2013, pp. 4259–4263.

[21] Minsu Cho and Kyoung Mu Lee, "Bilateral symmetry detection via symmetry-growing.," in *BMVC*, 2009.

[22] Martin Bokeloh, Alexander Berner, Michael Wand, H-P Seidel, and Andreas Schilling, "Symmetry detection using feature lines," in *Computer Graphics Forum*. Wiley Online Library, 2009, vol. 28, pp. 697–706.

[23] Hugo Cornelius and Gareth Loy, "Detecting bilateral symmetry in perspective," in *IEEE CVPR Workshops*. 2006, pp. 191–191.

[24] Pablo Arbelaez, Michael Maire, Charless Fowlkes, and Jitendra Malik, "Contour detection and hierarchical image segmentation," *IEEE Transactions on Pattern Analysis and Machine Intelligence*, vol. 33, no. 5, pp. 898–916, 2011.

[25] Jon Kleinberg and Eva Tardos, *Algorithm design*, Pearson Education India, 2006.

[26] Marcelo Cicconet, David GC Hildebrand, and Hunter Elliott, "Finding mirror symmetry via registration and optimal symmetric pairwise assignment of curves," in *IEEE ICCV Workshops*, 2017, pp. 1759–1763.